



## OPEN Bioinspired intratumoral infusion port catheter improves local drug delivery in the liver

Federico Pedersoli<sup>1</sup>, Imran Shair Mohammad<sup>2</sup>, Anup Kumar Patel<sup>2</sup>, Jonathan Kessler<sup>2</sup>, Cherng Chao<sup>2</sup>, Bo Liu<sup>2</sup>, Chandana Lall<sup>2</sup>, Catalina Guerra<sup>3</sup>, John J. Park<sup>4</sup> & F. Edward Boas<sup>2</sup>✉

Tumor immune modulation can be achieved using intratumoral injection of different immunomodulators during different phases of the cancer-immunity cycle. Intratumoral infusion catheters have been used in brain tumors, but these are not suitable outside the brain, where breathing motion results in catheter migration. Here, we use microstereolithography to manufacture a barbed sidehole catheter, modeled after the barbs in a bee stinger, where the barbs maintain the catheter position in the tumor, and sideholes within the barbs infuse drug into tumor tissue. In pig liver, we demonstrated 183-fold higher local drug concentration using the barbed sidehole catheter, compared to intravenous injection of water-soluble drug. High resistance sideholes and pulsatile injection both generate higher pressure in the catheter, which overcomes the tissue pressure, resulting in more drug delivery into tumor. A physical model of intratumoral infusion catheters accurately predicts the observed drug delivery results. Our catheter design is retained in the liver (and does not migrate out with breathing motion), and it preferentially infuses the drug into tumor tissue (not intratumoral vessels).

Intratumoral injection of immunotherapy agents<sup>1,2</sup> can be used to generate in situ cancer vaccines, resulting in abscopal effects, with regression of uninjected tumors<sup>3–9</sup>. Local delivery results in local drug concentrations that are hundreds to thousands of times higher than the systemic drug concentration<sup>10</sup>, enabling use of drugs that are too toxic or are ineffective when delivered systemically, such as vaccine adjuvants or cytokines.

However, daily intratumoral injections<sup>6–8,11</sup>, and complex dosing schedules involving different drugs at different time points<sup>3,9</sup> might be required to achieve the best results. For highly perfused liver tumors, the injected drug rapidly washes out into the systemic circulation. Thus, repeated injections can be required to generate sufficient immune stimulation.

Timed local delivery of different drugs during different phases of the cancer-immunity cycle<sup>12</sup>, from antigen presentation to effector cell recruitment and activation, could improve the anti-tumor immune response. Although the optimal timing is still unclear, some data suggests that immunosuppressive signals should be blocked before immunogenic cell death, T cell costimulation should occur after immunogenic cell death<sup>13,14</sup>, dendritic cells should be recruited to the tumor before they are activated<sup>3</sup>, and antigen presentation should be promoted before stimulating T cells<sup>9</sup>.

Repeated intratumoral injections have been performed in early phase human trials<sup>3,15,16</sup>, but are not practical for widespread use. To solve this problem, we designed and evaluated intratumoral infusion catheters, which are connected to subcutaneous ports. The catheter can be implanted in tumors in the liver and other organs. This allows for long-term intratumoral infusion of multiple drugs, using arbitrary dosing schedules, via the same type of subcutaneous port that is currently used for intravenous infusions.

We compare different mechanisms for retaining the infusion catheter in liver tumors, and also optimize the sidehole design to improve intratumoral drug delivery. The final optimized catheter design was inspired by the bee stinger, which has barbs to retain the stinger at the venom injection site.

### Results

The intrahepatic infusion catheter needs to perform two main functions: retention at the target site despite breathing motion, and uniform drug delivery into the target site. Two catheter designs were tested: a conventional multi-sidehole catheter with suture anchor retention, and a barbed sidehole catheter. Multiple sideholes are

<sup>1</sup>Interventional Radiology, Imaging Institute of Southern Switzerland (IIMSI), Ente Ospedaliero Cantonale (EOC), Locarno, Switzerland. <sup>2</sup>Department of Radiology / Interventional Radiology, City of Hope Medical Center, 1500 East Duarte Road, Duarte, CA 91010, USA. <sup>3</sup>Lundquist Institute, Torrance, CA, USA. <sup>4</sup>Harbor-UCLA Medical Center, Torrance, CA, USA. ✉email: fboas@coh.org

used to provide better coverage of larger tumors. The barbed sidehole infusion catheter has barbs to retain the catheter in the tumor, and high resistance sideholes in the barbs, to get more uniform drug delivery into the tumor (Fig. 1).

### Intrahepatic infusion port

Intrahepatic infusion port placement was technically successful, using a conventional multi-sidehole catheter, and suture anchor (Fig. 2). The suture anchor retains the catheter in the liver, in the setting of breathing motion. The subcutaneous port can be accessed with a Huber needle, and injected contrast is seen in the liver around the catheter tip.

### Barbed sidehole catheter

The barbed sidehole catheter was successfully printed using microstereolithography, which provides higher resolution than other 3D printing technologies (Fig. 3). Initial attempts using PolyJet or stereolithography were unsuccessful, due to insufficient resolution to produce the 0.4 mm sideholes. Microstereolithography properly resolves the barbs, sideholes, and central channel.

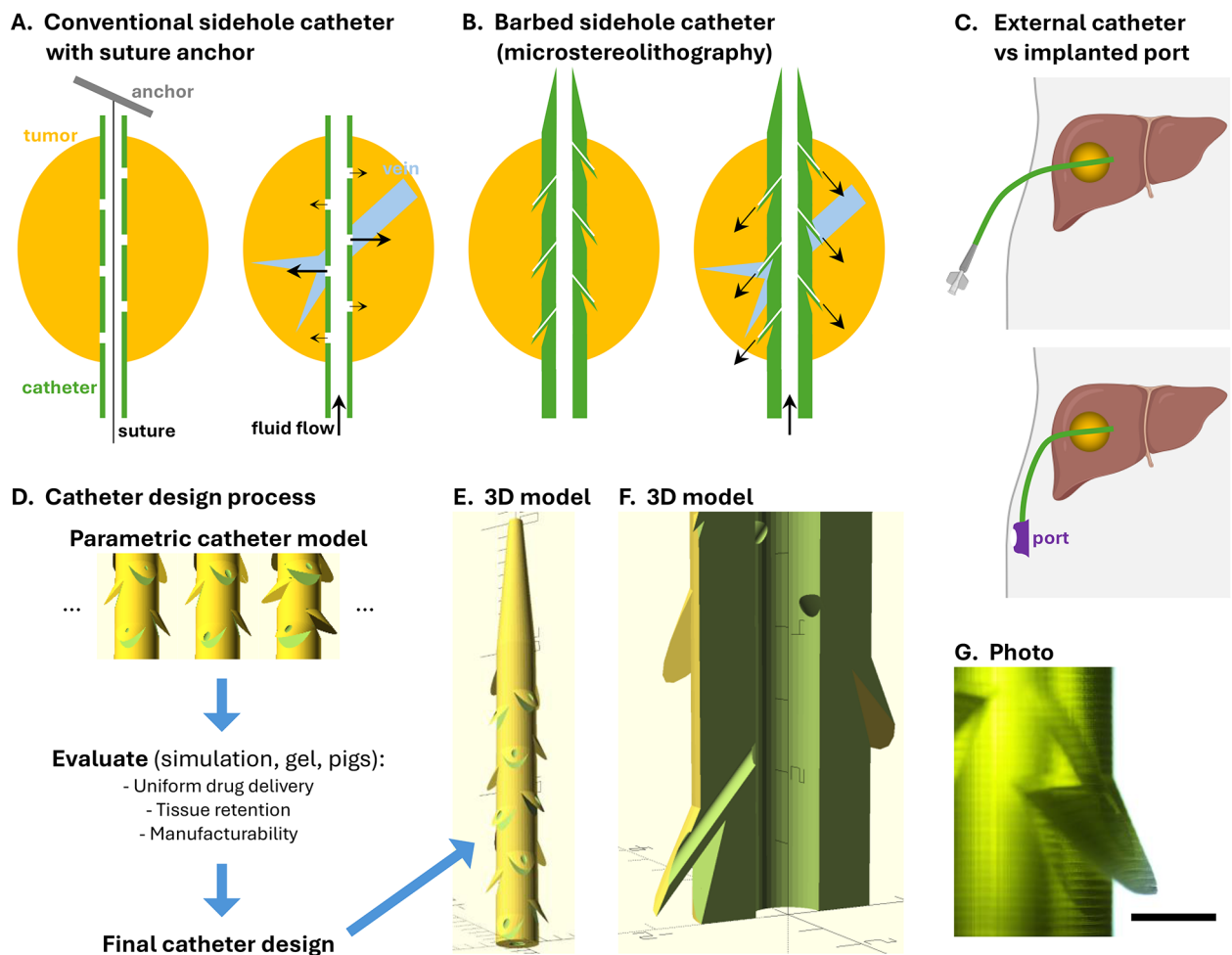


**Fig. 1.** Intratumoral infusion catheter designs. **A.** A conventional sidehole catheter can be retained in a tumor using an anchor attached to a suture in the catheter (the end of the suture is attached to the end of the catheter). Infused fluid preferentially flows into low pressure intratumoral veins. **B.** A barbed sidehole catheter has barbs that anchor the catheter to the tumor, and high resistance sideholes that regulate the flow rate, providing uniform drug delivery into the tumor. **C.** The intratumoral infusion catheter can have an external luer connector, or it can be connected to an implanted subcutaneous port. (Created with BioRender.com) **D.** Variations of the barbed sidehole catheter were evaluated to pick the optimal design. **E.** 3D model of the optimal catheter design, with tapered tip and barbs with side holes. **F.** Magnified cutaway view showing a side hole channel in a barb. The barb presses the sidehole into tumor tissue, and also prevents catheter migration. Each tick mark is 1 mm. **G.** Photomicrograph of a translucent 3D printed catheter, showing a barb with a sidehole connected to the central channel. Scale bar: 1 mm

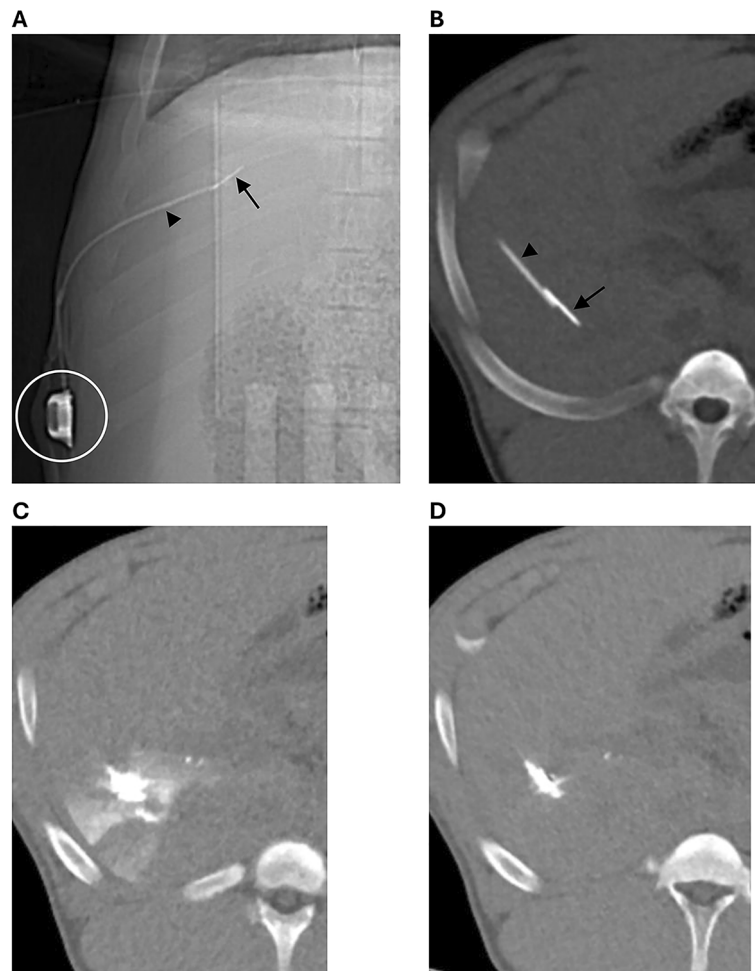


**Fig. 2.** Intrahepatic infusion catheter in a pig, attached to a subcutaneous port (circle), using a suture anchor (arrow) to retain the catheter (arrowhead) in the liver. The metal anchor in the liver is attached to a suture that goes through the catheter, and both the catheter and suture are attached to the port. **A.** Scout image. **B.** Thick slab CT showing the catheter tip and suture anchor in the liver. **C.** 0.5 min after contrast injection, contrast is seen in the liver around the catheter tip. **D.** 3.5 min after contrast injection, most of the contrast has washed out

### Pullout force

Force required to pull the catheter out of the liver was 7.6 N for the conventional sidehole catheter with suture anchor, and 5.3 N for the barbed sidehole catheter. Alternatively, if the suture is cut, the catheter can be pulled out with < 1 N force, leaving the anchor in the liver.

### Local drug delivery in gel

When injections are performed in liver tumors, some of the injected material stays in the tumor tissue, but some immediately goes into intratumoral veins. The goal of the intratumoral catheter is to maximize the amount of drug that is retained in tumor tissue. To evaluate this in vitro, we embed half of the sideholes in gel (to simulate tumor tissue), and half in saline (to simulate intratumoral veins), then inject dye, and measure the amount of dye in the gel, versus in saline.

The high-resistance barbed sidehole catheter resulted in 3.7-fold greater drug delivery into gel, compared to conventional sideholes ( $p=0.0098$ ). Pulsatile injection resulted in 51-fold greater drug delivery into gel, compared to continuous injection ( $p=0.012$ ). Pulsatile injection generates higher peak pressure and flow rate, at the same mean flow rate. See Figs. 4 and 5.

### Local drug delivery in pig liver

Compared to intravenous injection, pulsatile injection into the barbed sidehole catheter resulted in 183-fold higher local contrast retention, per mg iohexol injected. See Fig. 5.

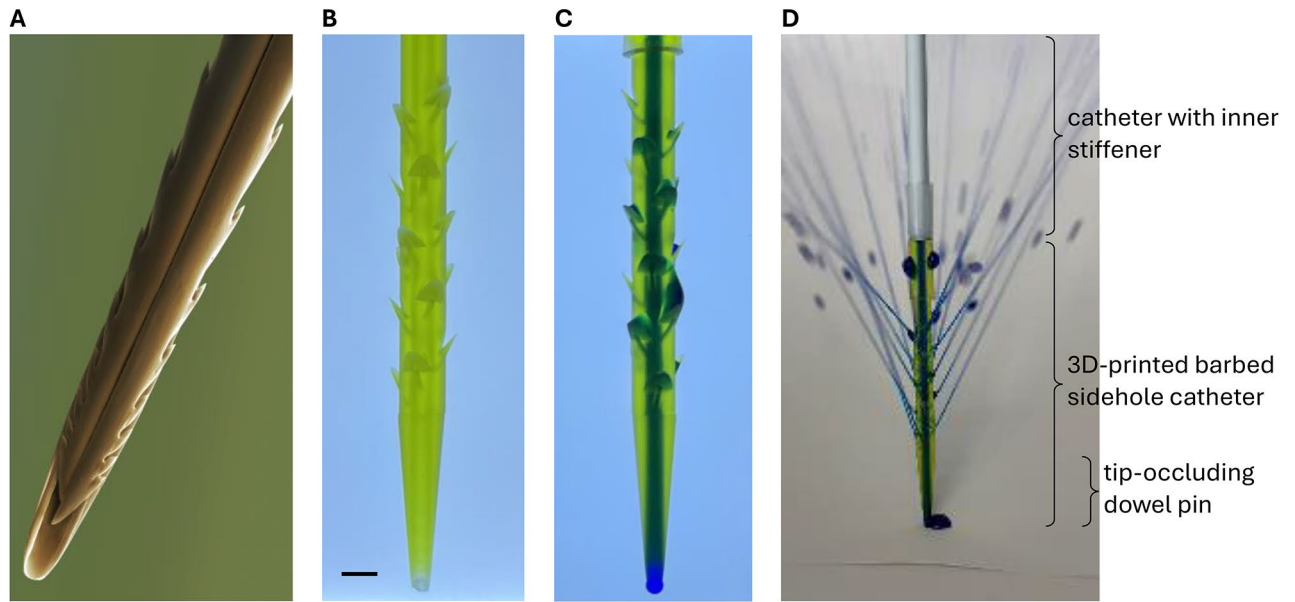


**Fig. 3.** Barbed sidehole catheter. The barbs retain the catheter in the tumor, and the sideholes allow intratumoral drug infusion. **A.** Colorized SEM image of a honey bee stinger, showing the barbs that retain the stinger at the venom injection site (Image credit: Power & Syred / Science Photo Library). **B.** Backlit photograph of the translucent barbed sidehole catheter. Scale bar: 2 mm. **C.** Methylene blue was injected into the catheter, to show the main catheter channel, as well as the sidehole channels. **D.** Fluid jets emerging from the barbed sidehole catheter.

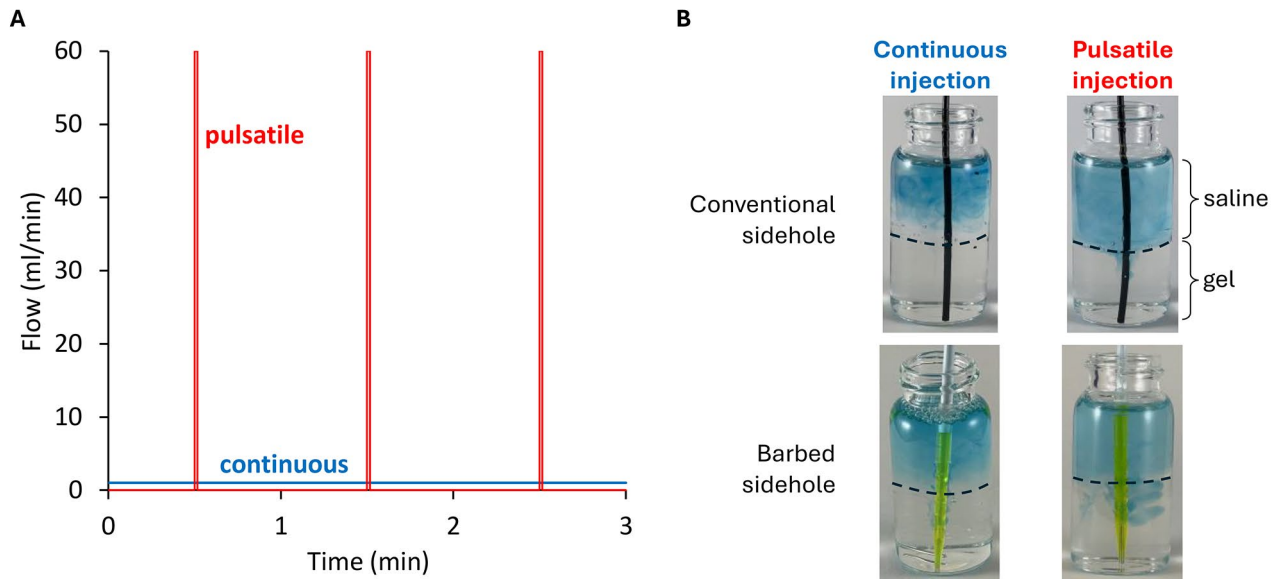


**Fig. 4.** Local drug delivery in gel. **A.** Mean flow rate is the same (1 ml/min) for both continuous and pulsatile injection. However, peak flow rate, pressure, and fluid jet velocity is much higher for pulsatile injection. **B.** Pulsatile injection through the barbed sidehole catheter results in the most dye in the gel.

**Physical model of intratumoral infusion**

When infusing drug through a multi-sidehole catheter into a tumor, some of the sideholes are in low resistance blood vessels, and some sideholes are embedded in tumor tissue. When the flow rate is low, or when sideholes are large, all of the fluid goes down the path of least resistance, which is into the veins, and not into the tumor (Fig. 1).

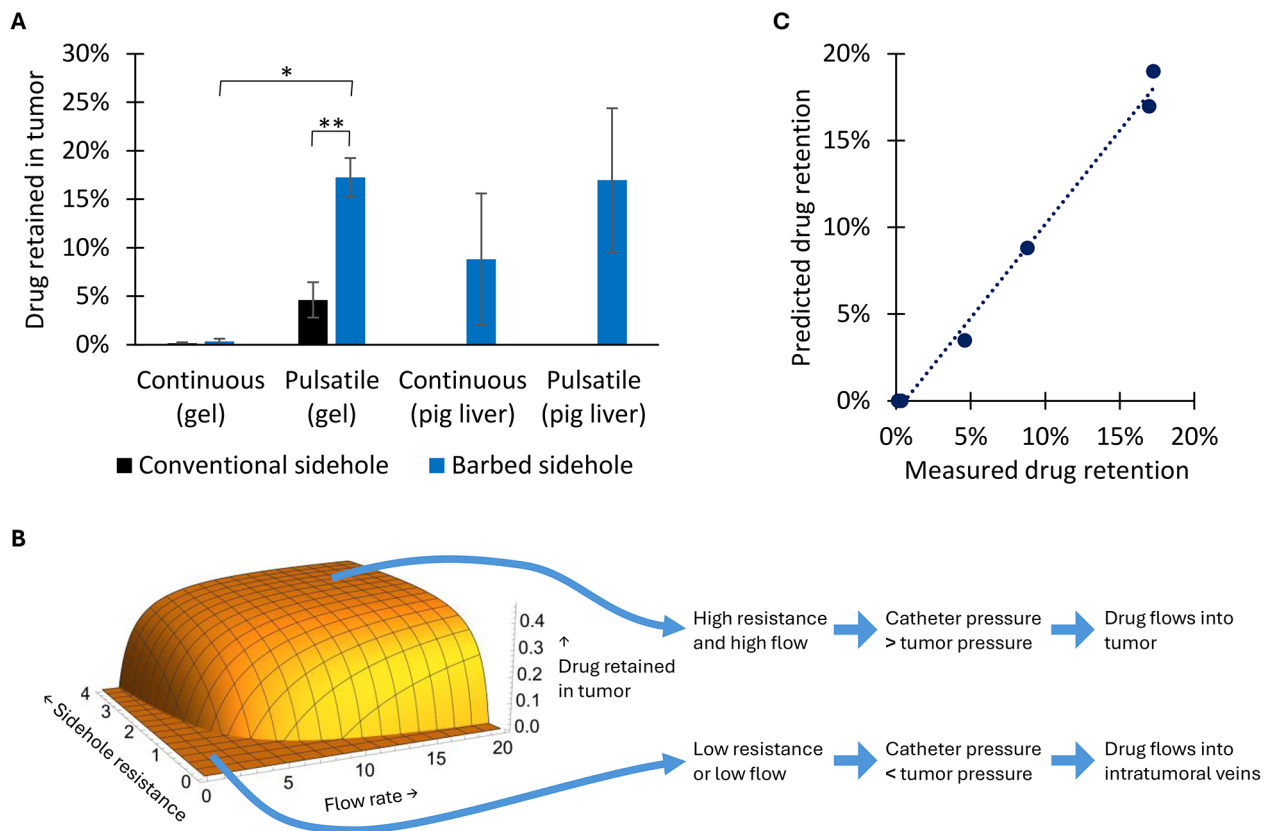


**Fig. 5.** Local drug delivery in gel and in pigs. **A.** Pulsatile injection into a high-resistance barbed sidehole catheter, results in the highest local drug retention. \* ( $p \leq 0.05$ ), \*\* ( $p \leq 0.01$ ) **B.** A physical model of intratumoral infusion through multi-sidehole catheters (see Supplemental Materials) predicts that higher flow rate, and higher sidehole resistance, results in higher intratumoral drug delivery. **C.** The physical model accurately predicts local drug retention in both gel and in pig liver.

Intratumoral drug delivery can be improved by increasing the sidehole resistance (for example, smaller sideholes), or by increasing the flow rate (for example, pulsatile flow). This results in higher pressure in the catheter, which overcomes the tissue pressure, resulting in more drug delivery into tumor. This physical model of intratumoral infusion is detailed in Supplemental Materials, and the model accurately predicts observed drug delivery both in vitro and in vivo (see Fig. 5).

## Discussion

Preclinical experiments and early phase human trials have shown that repeated intratumoral injection of immune stimulants, as well as complex dosing schedules involving different intratumoral drugs at different time points, can be required to generate good anti-tumor immune responses and abscopal effects. Unfortunately, repeated intratumoral injections increase the risk of procedural complications, and also place significant burdens on both the patient and the healthcare system. To address this problem, we have developed intratumoral infusion catheters, which can be implanted in tumors in the liver or other organs, and connected to subcutaneous ports. This enables long-term intratumoral infusion of multiple drugs, using arbitrary dosing schedules, performed at existing infusion centers.

There are two key design considerations for intratumoral infusion catheters. First, a retention mechanism is needed to prevent the catheter from migrating out of the liver with breathing motion. Here, we tested both a suture anchor, and barbs on the catheter. Both designs were sufficient for retaining the catheter at the target site in the liver. Pullout force was 43% higher for the suture anchor. However, the barbed catheter is easier to implant, because the retention mechanism is integrated into the catheter.

Second, the sideholes should be designed to maximize drug delivery into the tumor. Here, we compared conventional sideholes (created using a catheter punch) to smaller high resistance barbed sideholes (created in a 3D printer). The high resistance sideholes resulted in 3.7x greater local drug delivery. We also compared continuous and pulsatile injection. Pulsatile injection resulted in 51x greater local drug delivery. High resistance sideholes and pulsatile injection both generate higher pressure in the catheter, which overcomes the tissue pressure, resulting in more drug delivery into tumor. We developed a physical model of intratumoral infusion, which accurately predicts the observed drug delivery both in vitro and in vivo. This model can be used to guide the design of future intratumoral infusion catheters.

Optimal sidehole design is important for a wide range of medical and nonmedical applications, such as thrombolysis catheters and drip irrigation systems. The key challenge is to achieve uniform fluid delivery, and to prevent the fluid from preferentially flowing down the path of least resistance. For infusion into brain tumors, smaller sideholes have also been shown to improve drug delivery<sup>17</sup>. For thrombolysis catheters, side slits (which pop open in a pulsatile fashion during infusion) result in more uniform delivery of the thrombolysis agent into clot, compared to side hole catheters<sup>18</sup>.

To our knowledge, this paper is the first report of an intratumoral infusion catheter connected to a subcutaneous port. Multi-sidehole<sup>19</sup> and multi-pronged<sup>20</sup> needles have been designed for intratumoral injections, but those are used for single injections, and can not be implanted. Intratumoral infusion catheters have been placed in brain tumors, for infusion of oncolytic virus<sup>21</sup> or immunotherapy agents<sup>22</sup>. However, those are exterior catheters, not connected to a subcutaneous port. In addition, breathing motion is not an issue in the brain, so a retention mechanism is not required. An Ommaya reservoir is a subcutaneous port connected to a catheter in a lateral ventricle in the brain, and it has been used to deliver chemotherapy<sup>23</sup>, immunotherapy<sup>24</sup>, and cellular therapies<sup>25</sup> into the cerebrospinal fluid. Intraperitoneal catheters can be used to administer intraperitoneal chemotherapy<sup>26</sup> or immunotherapy<sup>27</sup>, for peritoneal metastases. Hepatic artery infusion pumps<sup>28</sup> can be placed by surgery, or percutaneous hepatic artery port catheters<sup>29,30</sup> can be placed by IR, for infusion of chemotherapy into liver tumors.

Future studies should address longer term stability and performance of these catheters, further optimization of the retention mechanism and sidehole geometry, and manufacturability, prior to translation into a human trial.

In conclusion, we have designed an intratumoral infusion port catheter that enables direct infusion of immunotherapy agents into tumors, using arbitrary dosing schedules. The catheter is retained in the liver (and does not migrate out with breathing motion), and it preferentially infuses the drug into tumor tissue. Microstereolithography can be used to produce catheters with unusual sidehole geometry. Smaller sideholes and pulsatile injection result in better local drug delivery. A physical model of intratumoral infusion catheters accurately predicts the observed drug delivery results.

## Methods

### Intrahepatic infusion port (conventional multi-sidehole catheter)

#### *Port design*

The basic strategy was to start with a standard intravenous port (PowerPort Slim Implantable Port with 6 F catheter, BD, Franklin Lakes, NJ), and modify it to enable intratumoral catheter placement. The subcutaneous port was used without modification. The polyurethane port catheter is too soft to easily advance into soft tissue, so we used a braided 5 F catheter instead (Impress Diagnostic Peripheral Catheter, Merit Medical, South Jordan, UT). A 20 G needle was used to punch 4 sideholes along the distal 1 cm of the catheter. A gastropexy suture anchor (Cope Gastrointestinal Suture Anchor Set, Cook Medical, Bloomington, IN) was used to anchor the catheter in the liver, to prevent it from migrating with breathing motion. Heat shrink tubing (McMaster-Carr, Elmhurst, IL) was used to connect the 5 F braided catheter to the 6 F polyurethane catheter, which was then attached to the port.

#### *Intrahepatic port placement (CT-guided)*

The Institutional Animal Care and Use Committee at the Lundquist Institute approved all research procedures. All experiments were performed in compliance with relevant guidelines and regulations, and ARRIVE guidelines were followed. All procedures and imaging were performed under general anesthesia. Euthanasia was performed by administering a barbiturate overdose intravenously, as per AVMA guidelines.

Under CT or ultrasound guidance, an 18 G Chiba needle was advanced into the target in the liver. The needle was exchanged over the back end of an Amplatz wire for a 5 F braided sidehole catheter. A gastropexy suture anchor was pushed through the 5 F catheter, into the liver, using a wire. The 5 F braided catheter was attached to the 6 F polyurethane catheter, using heat shrink tubing. The 6 F polyurethane catheter was then tunneled to the port pocket, where both the gastropexy suture and catheter were attached to the port reservoir. See Fig. 6.

### Barbed sidehole catheter

#### *Catheter design and manufacturing*

Using parametric CAD software (OpenSCAD), we designed the barbed sidehole catheter, with outer diameter 8 F, inner diameter 1 mm, 1 cm tapered tip, 18 sideholes from 1 to 3 cm from the tip, sidehole diameter 0.4 mm, and 40° angle between the sidehole channels and the main catheter channel. The parametric software enables easy modifications of the sidehole geometry, by changing the parameters (see Parametric catheter model in Supplemental materials).

The barbed sidehole infusion catheter was 3D printed at 10 micron resolution, using a microstereolithography printer (microArch S240, Boston Micro Fabrication, Maynard, MA), using biocompatible BMF MED resin. Only the catheter tip was 3D printed. The catheter tip was then attached to the end of a 6 F sheath (with the tip cut off), using heat shrink tubing, and using an 0.035" glidewire to align the lumens. The sheath serves as a catheter, plus an inner stiffener so that the catheter can be advanced through liver into the tumor. A stainless steel dowel pin (0.8 × 10 mm, McMaster-Carr) was used to occlude the endhole, so that the infusion goes through the sideholes only.

#### *Catheter placement into liver (CT-guided)*

Under CT or ultrasound guidance, an 18 G Chiba needle was advanced into the target in the liver. The needle was exchanged over the back end of an Amplatz wire for a dilator. The dilator was then exchanged over the wire

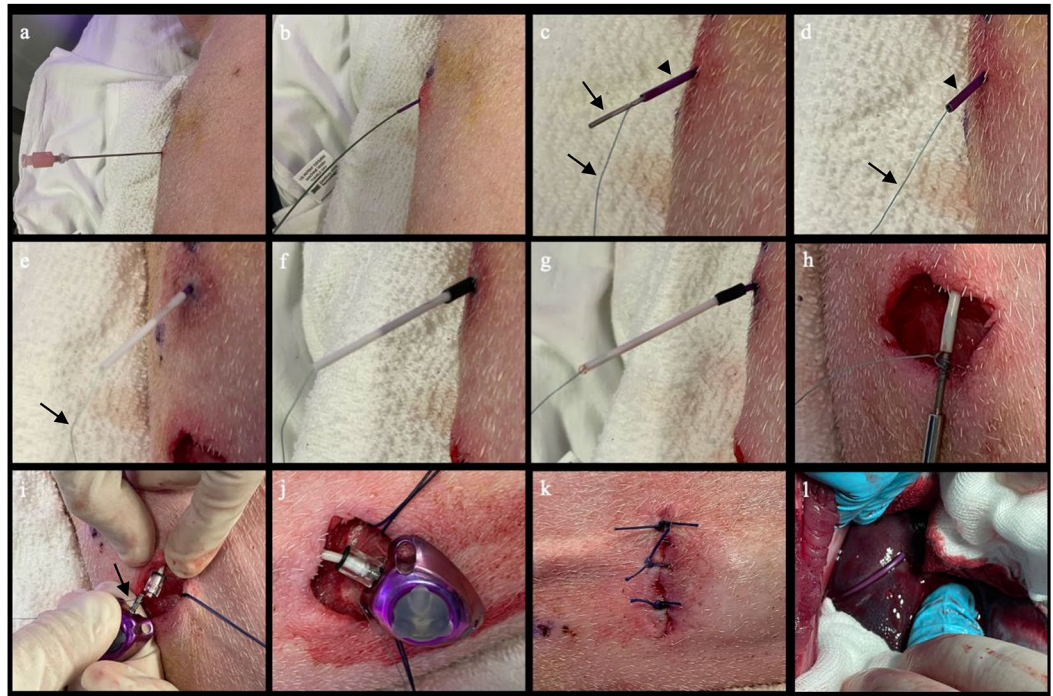


**Fig. 6.** Intrahepatic infusion port placement in a pig. **A.** Under CT or ultrasound guidance, an 18 G Chiba needle was advanced into the target in the liver. **B.** The needle was exchanged over the back end of an Amplatz wire for a 5 F braided sidehole catheter. **C & D.** A gastropexy suture anchor (arrows) was pushed through the 5 F catheter (arrowhead), into the liver, using a wire. **E.** The 5 F braided catheter and suture (arrow) were inserted into a 5 cm long 6 F polyurethane catheter (white). **F.** Heat shrink tubing (black) was placed across the two catheters. **G.** The tube was heated using a heat gun, to create a water-tight seal between the two catheters. **H.** The 6 F polyurethane catheter was connected to a tunneler, then tunneled to the subcutaneous port pocket. **I.** The suture (arrow) from the suture anchor was wrapped around the connector on the port reservoir, and then the 6 F polyurethane catheter was attached to the connector. **J & K.** The port reservoir was placed in the pocket, and the skin incision was closed. **L.** After port placement, necropsy shows the port catheter entering the liver.

for the barbed sidehole catheter. The steel dowel pin was pushed to the tip of the catheter, using the wire. The inner stiffener was then removed from the catheter.

#### Pullout force measurement

Both catheter designs (conventional sidehole with suture anchor retention, and barbed sidehole) were placed into pig liver *ex vivo*. Maximum pullout force (Newtons) was measured using a force meter.

#### Measuring local drug delivery in gel

Two catheters were tested: 1. the barbed sidehole catheter, and 2. a conventional 5 F sidehole catheter with 4 sideholes / cm. Sideholes were cut in the 5 F catheter using a catheter punch, with outer diameter 0.035" and inner diameter 0.025" (Syneo, Angleton, TX). Both catheters have a 1 cm tip with no sideholes, followed by 2 cm of sideholes. The endholes were occluded using steel dowel pins (0.8 × 10 mm).

Glass vials were filled with a 2 cm layer of 10% (w/v) hydroxypropyl methylcellulose (bottom), followed by a 2 cm layer of saline (top). Catheters were placed in the vials so that 1 cm of sideholes were in the bottom gel layer, and 1 cm of sideholes were in the top saline layer.

Methylene blue (0.02 mg/ml) was injected into the catheters. For continuous injections, 1 ml was injected over 1 min. For pulsatile injections, 0.5 ml was injected over 0.5 s, followed by a 59 s pause, followed by 0.5 ml injection over 0.5 s. Methylene blue in the bottom gel and top saline layers was measured by absorbance (see Quantitative Photography in Supplemental Materials). Experiments were performed in triplicate, and means were compared using two-tailed *t*-tests.

#### Measuring local drug delivery in pigs

Barbed and conventional sidehole catheters were placed in the livers of 3 Yorkshire pigs. Iohexol (276 mg/ml) was injected into the catheters, and CT of the liver was performed 30 s after completing the injections. For continuous injections, 3 ml was injected over 1 min. For pulsatile injections, 1.5 ml was injected over 0.5 s, followed by a 59 s pause, followed by 1.5 ml injection over 0.5 s. The iohexol concentration was selected to stay under the maximum Hounsfield units (HU) for the CT scanner. Iohexol (276 mg/ml) is 2233 HU at 120 kVp,

compared to the maximum HU of 3071 (which is due to the 12-bit DICOM files, which can store HU values ranging from  $-1024$  to  $3071$ ).

To quantify iohexol retention at the injection site, a 3D region of interest (ROI) was drawn around the injection site, and the volume and mean HU of the ROI was measured. HU of a mixture is linearly related to the HU of the components of the mixture. Thus:  $HU_{ROI} = \nu HU_{contrast} + (1-\nu) HU_{liver}$ , where  $\nu$  is the fraction of the ROI volume that contains contrast. Therefore, the volume of contrast in the ROI is:  $Volume_{ROI} \times (HU_{ROI} - HU_{liver}) / (HU_{contrast} - HU_{liver})$ .

To measure maximum iohexol delivery into liver from intravenous administration, 120 ml of Omnipaque 300 was administered intravenously, and multiphase CT of the liver was obtained, and the maximum enhancement of the liver parenchyma was measured.

## Data availability

The 3D model of the barbed sidehole catheter is provided in Supplementary materials.

Received: 12 September 2024; Accepted: 11 November 2024

Published online: 13 November 2024

## References

- Murthy, R. et al. 397 intra-tumor immunotherapy injections utilizing image guidance in interventional radiology: clinical trial experience at a tertiary care cancer center. *J. Immunother. Cancer*. **8**, A241–A242. <https://doi.org/10.1136/jitc-2020-SITC2020.0397> (2020).
- Shyr, C. R., Liu, L. C., Chien, H. S. & Huang, C. P. Immunotherapeutic agents for Intratumoral Immunotherapy. *Vaccines (Basel)*. **11** <https://doi.org/10.3390/vaccines11111717> (2023).
- Hammerich, L. et al. Systemic clinical tumor regressions and potentiation of PD1 blockade with in situ vaccination. *Nat. Med.* <https://doi.org/10.1038/s41591-019-0410-x> (2019).
- Som, A. et al. Percutaneous Intratumoral Immunoadjuvant Gel increases the Abscopal Effect of Cryoablation for checkpoint inhibitor resistant Cancer. *Adv. Healthc. Mater.* **13**, e2301848. <https://doi.org/10.1002/adhm.202301848> (2024).
- Ghani, M. A. et al. Treatment of Hepatocellular Carcinoma by Multimodal In Situ Vaccination Using Cryoablation and a Plant Virus Immunostimulant. *J. Vasc. Interv. Radiol.* **34**, 1247–1257 e1248, doi: (2023). <https://doi.org/10.1016/j.jvir.2023.03.016>
- Hong, W. X., Sagiv-Barfi, I., Czerwinski, D. K., Sallets, A. & Levy, R. Neoadjuvant Intratumoral Immunotherapy with TLR9 activation and Anti-OX40 antibody eradicates metastatic Cancer. *Cancer Res.* **82**, 1396–1408. <https://doi.org/10.1158/0008-5472.CAN-21-1382> (2022).
- Anfray, C. et al. Intratumoral combination therapy with poly(I:C) and resiquimod synergistically triggers tumor-associated macrophages for effective systemic antitumoral immunity. *J. Immunother. Cancer.* **9** <https://doi.org/10.1136/jitc-2021-002408> (2021).
- Chu, Y. et al. Tumor eradicated by combination of imiquimod and OX40 agonist for in situ vaccination. *Cancer Sci.* **112**, 4490–4500. <https://doi.org/10.1111/cas.15145> (2021).
- Zhang, Y. et al. In situ Vaccination following intratumoral injection of IL2 and Poly-L-lysine/Iron Oxide/CpG nanoparticles to a Radiated Tumor Site. *ACS Nano.* **17**, 10236–10251. <https://doi.org/10.1021/acsnano.3c00418> (2023).
- Boas, F. E. et al. Bronchial or pulmonary artery chemoembolization for unresectable and unablatable lung metastases: a phase I clinical trial. *Radiology.* **301**, 474–484. <https://doi.org/10.1148/radiol.2021210213> (2021).
- Moreira, D. et al. Myeloid cell-targeted STAT3 inhibition sensitizes head and neck cancers to radiotherapy and T cell-mediated immunity. *J. Clin. Invest.* **131** <https://doi.org/10.1172/JCI137001> (2021).
- Chen, D. S. & Mellman, I. Oncology meets immunology: the cancer-immunity cycle. *Immunity.* **39**, 1–10. <https://doi.org/10.1016/j.immuni.2013.07.012> (2013).
- Gunderson, A. J. & Young, K. H. Exploring optimal sequencing of radiation and immunotherapy combinations. *Adv. Radiat. Oncol.* **3**, 494–505. <https://doi.org/10.1016/j.adro.2018.07.005> (2018).
- Young, K. H. et al. Optimizing timing of Immunotherapy improves control of tumors by Hypofractionated Radiation Therapy. *PLoS One.* **11**, e0157164. <https://doi.org/10.1371/journal.pone.0157164> (2016).
- Marron, T. et al. Flt3L-primed in situ vaccination and pembrolizumab induce systemic tumor regressions of bulky tumors in patients with lymphomas and ER/PR+ breast cancer. *J. Immunother. Cancer.* **10** <https://doi.org/10.1136/jitc-2022-SITC2022.0595> (2022).
- Meric-Bernstam, F. et al. Phase I dose-escalation trial of MIW815 (ADU-S100), an Intratumoral STING agonist, in patients with Advanced/Metastatic Solid tumors or lymphomas. *Clin. Cancer Res.* **28**, 677–688. <https://doi.org/10.1158/1078-0432.CCR-21-1963> (2022).
- D'Amico, R. S., Aghi, M. K., Vogelbaum, M. A. & Bruce, J. N. Convection-enhanced drug delivery for glioblastoma: a review. *J. Neurooncol.* **151**, 415–427. <https://doi.org/10.1007/s11060-020-03408-9> (2021).
- Cho, K. J. & Recinella, D. K. Pattern of dispersion from a pulse-spray catheter for delivery of thrombolytic agents: design, theory, and results. *Acad. Radiol.* **4**, 210–216. [https://doi.org/10.1016/s1076-6332\(05\)80293-4](https://doi.org/10.1016/s1076-6332(05)80293-4) (1997).
- Munoz, N. M. et al. Influence of injection technique, drug formulation and tumor microenvironment on intratumoral immunotherapy delivery and efficacy. *J. Immunother. Cancer.* **9** <https://doi.org/10.1136/jitc-2020-001800> (2021).
- Kuang, M. et al. Ethanol ablation of hepatocellular carcinoma up to 5.0 cm by using a multipronged injection needle with high-dose strategy. *Radiology.* **253**, 552–561. <https://doi.org/10.1148/radiol.2532082021> (2009).
- Friedman, G. K. et al. Oncolytic HSV-1 G207 immunovirotherapy for Pediatric High-Grade Gliomas. *N. Engl. J. Med.* **384**, 1613–1622. <https://doi.org/10.1056/NEJMoa2024947> (2021).
- Sperring, C. P. et al. Convection-enhanced delivery of immunomodulatory therapy for high-grade glioma. *Neurooncol. Adv.* **5**, vdad044. <https://doi.org/10.1093/oaajnl/vdad044> (2023).
- Zubair, A. & De Jesus, O. in *StatPearls* (2024).
- Jung, G. et al. Local immunotherapy of glioma patients with a combination of 2 bispecific antibody fragments and resting autologous lymphocytes: evidence for in situ t-cell activation and therapeutic efficacy. *Int. J. Cancer.* **91**, 225–230. [https://doi.org/10.1002/1097-0215\(200002\)9999:9999%3C:AID-IJC1038%3E3.0.CO;2-G](https://doi.org/10.1002/1097-0215(200002)9999:9999%3C:AID-IJC1038%3E3.0.CO;2-G) (2001).
- Clemons-Miller, A. R. et al. Intrathecal cytotoxic T-cell immunotherapy for metastatic leptomeningeal melanoma. *Clin. Cancer Res.* **7**, 917s–924s (2001).
- van Driel, W. J. et al. Hyperthermic Intraperitoneal Chemotherapy in Ovarian Cancer. *N. Engl. J. Med.* **378**, 230–240. <https://doi.org/10.1056/NEJMoa1708618> (2018).
- Morano, W. F. et al. Intraperitoneal immunotherapy: historical perspectives and modern therapy. *Cancer Gene Ther.* **23**, 373–381. <https://doi.org/10.1038/cgt.2016.49> (2016).
- Thiels, C. A. D'Angelica, M. I. Hepatic artery infusion pumps. *J. Surg. Oncol.* **122**, 70–77. <https://doi.org/10.1002/jso.25913> (2020).



29. Deschamps, F. et al. Intra-arterial hepatic chemotherapy: a comparison of percutaneous versus surgical implantation of port-catheters. *Cardiovasc. Intervent Radiol.* **34**, 973–979. <https://doi.org/10.1007/s00270-010-9996-6> (2011).
30. Chevallier, O. et al. Percutaneous implantation of a microcatheter-Port System for Hepatic Arterial Infusion Chemotherapy of Unresectable Liver Tumors: technical feasibility, functionality, and complications. *Diagnostics (Basel)*. **11** <https://doi.org/10.3390/diagnostics11030399> (2021).

## Acknowledgements

This research was funded by City of Hope and NIH/NCI (P30CA033572 and UM1 CA186717). 3D printing services were provided by Boston Micro Fabrication.

## Author contributions

FP, IM, AP, and FB performed experiments. FP and FB wrote the manuscript, and all authors reviewed the manuscript.

## Declarations

## Competing interests

FEB received research grants from City of Hope, Guerbet, Society of Interventional Radiology, Society of Interventional Oncology, Department of Defense, Thompson family foundation, and Brockman Medical Research Foundation. He received research supplies (investigator-initiated) from Boston Scientific, and attended a research consensus panel with the Society of Interventional Oncology. He is a shareholder in City of Hope Medical Group, co-founder of Claripacs, LLC, and an investor in Labdoor, Qventus, CloudMedx, Xgenomes, and Solugen. He is the inventor and assignee on US patent 8233586, and the inventor on US Patent Appl. 18/607,972. A patent application covering the intratumoral infusion port catheter is planned. JK received a grant from Metavivor, and consulting fees from Johnson and Johnson, Boston Scientific, and Galvanize Therapeutics. CC received support for attending meetings from Boston Scientific and Stryker. BL is a consultant for Sirtex Medical Limited. JJP is a proctor for Sirtex, and is on a medical advisory board for Boston Scientific. The other authors did not have any competing interests.

## Additional information

**Supplementary Information** The online version contains supplementary material available at <https://doi.org/10.1038/s41598-024-79694-4>.

**Correspondence** and requests for materials should be addressed to F.E.B.

**Reprints and permissions information** is available at [www.nature.com/reprints](http://www.nature.com/reprints).

**Publisher's note** Springer Nature remains neutral with regard to jurisdictional claims in published maps and institutional affiliations.

**Open Access** This article is licensed under a Creative Commons Attribution-NonCommercial-NoDerivatives 4.0 International License, which permits any non-commercial use, sharing, distribution and reproduction in any medium or format, as long as you give appropriate credit to the original author(s) and the source, provide a link to the Creative Commons licence, and indicate if you modified the licensed material. You do not have permission under this licence to share adapted material derived from this article or parts of it. The images or other third party material in this article are included in the article's Creative Commons licence, unless indicated otherwise in a credit line to the material. If material is not included in the article's Creative Commons licence and your intended use is not permitted by statutory regulation or exceeds the permitted use, you will need to obtain permission directly from the copyright holder. To view a copy of this licence, visit <http://creativecommons.org/licenses/by-nc-nd/4.0/>.

© The Author(s) 2024